CHEMISTRY OF MATERIALS

Article

pubs.acs.org/cm

Osmotic-Pressure-Mediated Control of Structural Colors of Photonic Capsules

Tae Min Choi,[†] Jin-Gyu Park,[‡] Young-Seok Kim,[§] Vinothan N. Manoharan,[‡] and Shin-Hyun Kim*,[†]

[†]Department of Chemical and Biomolecular Engineering and KINC, KAIST, Daejeon 305-701, South Korea

[‡]School of Engineering and Applied Sciences and Department of Physics, Harvard University, Cambridge, Massachusetts 02138, United States

[§]Korea Electronics Technology Institute, Seongnam-si, Gyeonggi-do 463 816, South Korea

W *Web-Enhanced Feature* *S* *Supporting Information*

ABSTRACT: Crystalline or glassy materials made of colloidal nanoparticles show distinctive photonic effects; the crystals exhibit sparkling colors with strong iridescence, while the glasses show noniridescent colors. Both colors are the results of constructive interference of the reflected light by the nonadsorbing nanostructures. Such colored materials have potential applications as nonfading colorants in reflective color displays, optical sensors, coatings, and cosmetics. All of these applications require granular format of the nanostructures; however, precise control of the nanostructures from amorphous to crystalline over the submillimeter length scale remains challenging. Here, we present micrometer-level control of photonic nanostructures confined in microcapsules through osmotic-pressure-mediated concentration. We encapsulate aqueous suspensions of colloidal particles using double-emulsion drops with ultrathin layers of photocurable resin. The microcapsules are then isotropically compressed by imposing a positive osmotic pressure difference that forces the water out through the thin resin membrane. We find that the internal nanostructure of our photonic microcapsules can be kinetically controlled from crystalline to amorphous; slow concentration in small pressure gradients yields colloidal crystals with sparkling color patterns, whereas fast concentration in large pressure gradients yields glassy packing with only short-range order, which show uniform color with little iridescence. By polymerizing the thin monomeric shell, we permanently fix these nanostructures. Our findings provide new insights into the design and synthesis of optical materials with controlled structural colors.

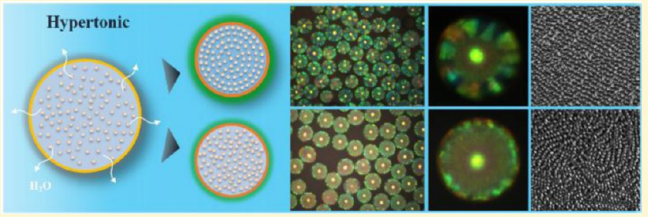

INTRODUCTION

Periodic colloidal nanostructures on the scale of half the wavelength of visual light show reflected colors, because of the constructive interference of selected wavelengths of light.[1] Such structural colors are distinguished from the usual "chemical colors" that arise from absorption spectra. When the colloidal nanostructures have long-range order, the color is iridescent;[2] when the order is short-ranged, the color is noniridescent and isotropic.[3] Although most chemical colors eventually fade, because of the oxidation or reaction of their chemical structures, structural colors can persist for as long as their periodic structures survive. Moreover, the structural colors can be dynamically tuned by controlling the periodicity of the nanostructures through chemical environment, temperature, and electric fields.[4] These unique properties of structural colors make them appealing for many applications, including colorimetric sensors, pigments, and reflection-mode displays.[4,5]

Structurally colored pigments have been produced using emulsion drops to confine colloidal assembly;[6−11] the resulting pigments can be assembled to build photonic devices or can be dispersed in liquid media to make paints. Single-emulsion drops yield consolidated granules of colloidal crystals through solvent evaporation,[7] and double-emulsion drops enable the colloidal structures to be encapsulated in a liquid state, forming photonic capsules protected by a solid membrane;[8] colloidal assemblies are sometimes nested in a shell of double-emulsion drops to form photonic shell structures.[9] These double-emulsion drops can be further compressed by imposing osmotic pressure, allowing for post-fabrication control of the structural colors.[10,11] Various types of particles can be used: charged nanoparticles tend to form highly ordered crystalline arrays whose color can be adjusted by osmotic pressure,[10] whereas soft hydrogel nanoparticles naturally pack into dense amorphous structures that show noniridescent color that can be tuned in a similar manner.[11] However, the relationship between the internal nanostructure of the microcapsules and the strength and rate of compression is still not understood. This is one of the critical design criteria for achieving nonfading photonic materials with controlled optical properties.

In this article, we report a facile microfluidic approach to create photonic ink capsules with controlled internal structure and interference color. With a capillary microfluidic device, we prepare water-in-oil-in-water (W/O/W) double-emulsion drops consisting of a colloidal particle-laden core and an ultrathin

Received: November 24, 2014
Revised: January 12, 2015
Published: January 14, 2015

DOI: 10.1021/cm5043292
Chem. Mater. 2015, 27, 1014−1020

photocurable shell. Under hypertonic conditions, the osmotic pressure difference selectively pumps water out across the shell, thereby concentrating the colloid in the core. Such nanostructures can be permanently fixed by photopolymerizing the shell, yielding stable photonic ink capsules. We find that the applied osmotic pressure gradient dramatically affects the internal nanostructures of the ink capsules. In small osmotic pressure gradients, the particles are slowly concentrated and assemble into crystal structures. By contrast, in high osmotic pressure gradients, the particles are rapidly concentrated and their nanostructure becomes amorphous. This is due to the dynamic arrest of the particles triggered by the sudden increase in volume fraction. The ability to tune the internal nanostructures makes it possible to control the iridescence of the photonic microcapsules. Stepwise increase of osmotic pressure results in a highly ordered array with sparkling iridescent colors, whereas sudden concentration results in amorphous packing of particles and a subsequent non-iridescent color.

RESULTS AND DISCUSSION

Microfluidic Preparation of Double-Emulsion Droplets. As a template for the photonic capsules, we prepare W/O/W double-emulsion drops with ultrathin shells using a capillary microfluidic device. The device is composed of two tapered cylindrical capillaries that are assembled in a square capillary, as shown in Figure 1a. One cylindrical capillary with a 100-μm orifice is rendered hydrophobic and used for injecting fluids, whereas the other one, with a 200-μm orifice, is rendered hydrophilic and used to collect drops. Another small tapered capillary is inserted into a wide opening of the hydrophobic capillary[11] (see the Experimental Section for details of device preparation). The innermost phase, containing 5% v/v monodisperse polystyrene (PS) particles and 2% w/w poly(vinyl alcohol) (PVA) in distilled water, is injected through the small capillary, and a photocurable middle phase of ethoxylated trimethylolpropane triacrylate (ETPTA) containing 1% w/w photoinitiator is injected through the hydrophobic injection capillary. The hydrophobicity of the injection capillary forces the aqueous suspension of PS particles to flow through the center of the capillary in the form of plug-shaped drops that do not contact the wall, while the middle phase completely wets the wall and flows along it. This core−sheath flow is emulsified into the third continuous phase of 10% w/w PVA in distilled water at the tip of the injection capillary, producing double-emulsion drops with ultrathin shells, as shown in Figure 1b and Movie S1 in the Supporting Information; the shell thickness is estimated as 0.2 μm. Although some single oil drops are co-produced, because of the oil between the pluglike drops, they are easily separated from the double-emulsion drops by exploiting their density difference; single oil drops rapidly sediment, because of their large density of 1.101, while the thin-shelled double-emulsion drops slowly sediment, because of small density difference with the continuous phase.[12] The small orifice of the collection capillary facilitates the flow-focusing into the capillary and exerts a large drag force on the hanging drop at the tip of the injection capillary. Therefore, this enables the breakup of interface at relatively low volumetric flow rate of the continuous phase. The resulting double-emulsion drops flow through the collection capillary, as shown in Figure 1c.

Concentration of Colloids under Hypertonic Conditions and Solidification of Membrane. Double-emulsion drops are incubated in aqueous solutions of NaCl and PVA, where the concentration of PVA is set to be 2% w/w and the concentration of NaCl is varied between 0.05 and 0.22 M to control the osmolarity of the solution; PVA is used for stabilization of outermost interface of double-emulsion drops. Under hypertonic conditions, meaning that the osmolarity of the incubation solution is higher than that of the drop cores, water in the core is selectively pumped out through the ultrathin shell, shrinking the droplet isotropically and concentrating the colloid, as illustrated in Figure 1d. The thinness of the shell facilitates transport of water, making it possible to precisely control the shrinkage rate.[10a] Moreover, the strong lubrication resistance in the thin film of liquid retards the movement of the core drops and prolongs the lifetime of the double-emulsion drops;[13] double-emulsion drops with shells $\geq$4 μm thick of the same material composition all rupture under the same incubation conditions. During the compression, the volume fraction of colloidal particles inside the double-emulsion droplets increases. The nanoparticles order, and the capsule develops structural color. We then solidify the thin shell of ETPTA by polymerizing with ultraviolet (UV) irradiation, as schematically shown in Figure 1d. When we incubate double-emulsion drops with diameters of 140 μm containing PS particles with diameters of 156 nm in a hypertonic incubation solution of 180 mOsm L^{-1} for 2 h, the drops are compressed to a diameter of 80 μm, as shown in

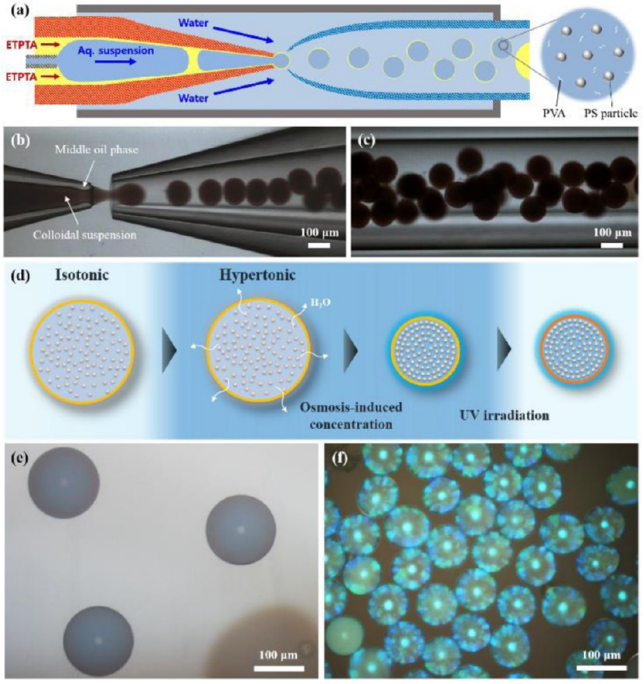

Figure 1. (a) Schematic illustration of a glass capillary microfluidic device for preparation of water-in-oil-in-water (W/O/W) double-emulsion droplets with an ultrathin middle layer. The innermost aqueous droplets contain monodisperse polystyrene (PS) particles and poly(vinyl alcohol) (PVA), and the middle oil layer is a photocurable resin of ethoxylated trimethylolpropane triacrylate (ETPTA). (b, c) Optical microscope images showing generation of double-emulsion droplets at the tip of the injection capillary and their downstream motion in the device. (d) A series of animations illustrating osmotic-pressure-induced concentration of colloidal particles confined in double-emulsion drops and subsequent solidification of the middle layer by UV-induced photopolymerization; this yields a photonic capsule. (e, f) Optical microscope images of double-emulsion droplets under isotonic conditions and photonic capsules prepared by concentration and shell solidification. Both images are taken in reflection mode, and their scales are set to be same for size comparison.

DOI: 10.1021/cm5043292
Chem. Mater. 2015, 27, 1014−1020

Figures 1e and 1f. The initial double-emulsion drops do not display any color, because of the lack of order in the colloid; although colloids with high surface charge density form crystals due to electrostatic repulsion,[8a] colloids dispersed in PVA solution have low surface charge density and do not form crystals at low volume fraction. However, they develop pronounced structural color with sparkling patterns during the compression. The color and internal structure remain intact during photopolymerization of ETPTA in the shell and even after the microcapsules are transferred to distilled water, showing that the polymerized ETPTA is sufficiently rigid to resist the imposed negative osmotic stress.

Influence of Particle Size on Structural Color. When the particles are concentrated, they form hexagonal arrays along the entire inner wall of the core, and a face-centered cubic (fcc) structure grows from the surface.[10a] Therefore, the microcapsules exhibit structural colors arising from reflections from the stacked (111) planes of the fcc lattice. The stop band position (λ) of the L-gap associated with reflections from the (111) planes can be estimated from Bragg's law:[14]

$$\lambda = 2dn_{\text{eff}} = \left(\frac{\pi}{3\sqrt{2}\phi}\right)^{1/3}\left(\frac{8}{3}\right)^{1/2} D\{n_{\text{PS}}{}^2\phi + n_{\text{water}}{}^2(1-\phi)\}^{1/2} \quad (1)$$

where d is the (111) plane spacing, D the particle diameter, and ϕ the particle volume fraction. The effective refractive index (n_{eff}) is calculated from the Maxwell−Garnett average of the refractive indices of PS and water (n_{PS} and n_{water}, respectively). The wavelength of the structural color can be adjusted by varying either the particle size or volume fraction according to eq 1.

To investigate the influence of particle size, we encapsulate three different suspensions of PS particles with diameters of 156, 191, and 222 nm. The initial volume fraction is set to 5% v/v for all of the suspensions. The three different double-emulsions are incubated in an aqueous solution with low osmolarity (180 mOsm L^{-1}) for 2 h, over which time the particles are gradually concentrated, arriving at the same final volume fraction. The resulting microcapsules display sparkling color patterns, as shown in Figures 2a−c, indicating crystal formation. Each microcapsule has a bright dot at the center and color patches along the edge. The central dot comes from normal reflection at the L-gap, while the side color patches come from reflections from the other crystal planes.[8a] The structural color varies significantly with the particle diameter, as shown by reflectance spectra of single photonic microcapsule in Figure 2d. Assuming that the color is due to the L-gap, we can estimate the particle volume fraction from the reflectance peak using eq 1. We find that ϕ = 0.297 for D = 222 nm, 0.295 for 191 nm, and 0.294 for 156 nm. The data show that constant osmotic pressure leads to (i) a constant and well-controlled final volume fraction, and (ii) a wavelength for the structural color that scales linearly with the particle size.

Influence of External Osmotic Pressure on Photonic Capsules. The structural color of the microcapsule is also influenced by the particle volume fraction. We compress droplets containing a 5% v/v aqueous suspension of PS particles (D = 191 nm) under three different osmotic pressures: 180, 300, and 440 mOsm L^{-1}. These imposed pressures lead to three different volume fractions. In addition, because the rate of concentration also varies with the imposed osmotic pressure gradient, ordering of the particles varies between these three samples. To study the influence of both final volume fraction and concentration rate, we observe the double-emulsion drops as they shrink using an optical microscope, as shown in Figures 3a and 3b (the full series of images are shown in Figure S1 in the Supporting Information and Movie S2). Upon incubation in a solution with 180 mOsm L^{-1}, the drop slowly shrinks and starts to show red color after 10 min, as shown in Figure 3a. Then, a crystal forms along the inner wall of the core after 20 min, as evidenced by the appearance of a central dot and thin color patches at the edge in the second image; the onset of crystallization is observed at t = 797 s, as shown in Figure S1a in the Supporting Information. The crystal then grows toward the center of the core as shown in the last of images: the central dot becomes brighter and the color patches become thicker. By contrast, droplets incubated at 440 mOsm L^{-1} rapidly shrink and display no color patches. Instead, these shrunken drops develop a homogeneous green color as shown in Figure 3b. We attribute this to the formation of amorphous glassy structures with short-range order, because of kinetic or dynamic arrest; that is, the crystallization appears to be suppressed by fast concentration.[15] Monodisperse photonic capsules prepared at three different osmolarities of 180, 300, and 440 mOsm L^{-1} are shown in Figures 3c−e. We find that the degree of crystallization, as determined by the size of the color patches, is reduced as the osmotic pressure difference increases; a weakly sparkling color ring appears in the edge of capsules in Figures 3d and 3e, which indicates the formation of a thin layer of crystalline structure in the outermost part of the capsule. The osmotic pressure of the incubation solution also influences the final volume fraction of the particles. We see this from the blue shift of the structural colors as the osmotic pressure difference increases.

The evolution of particle volume fraction ϕ over the incubation time t from the initial value ϕ_0 can be estimated from the radius of the drop $R(t)$ and the thickness of the shell $l(t)$, which have initial values R_0 and l_0:

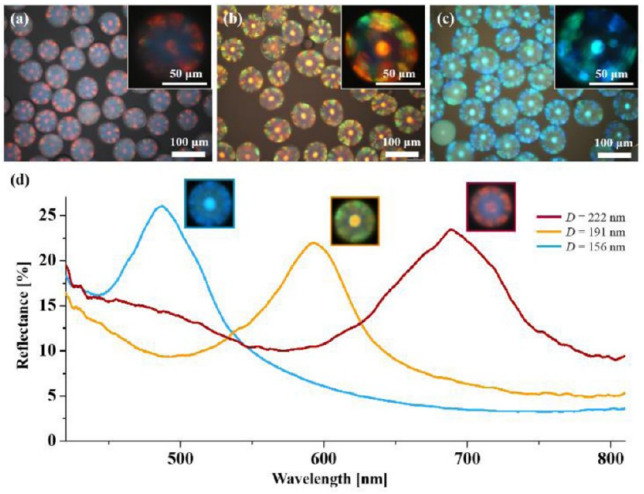

Figure 2. (a-c) Optical microscope images of photonic capsules containing colloidal crystals of monodisperse PS particles with diameters of (a) 222 nm, (b) 191 nm, and (c) 156 nm, where all double-emulsion drops are incubated in an aqueous solution with an osmolarity of 180 mOsm L^{-1} for 2 h prior to photopolymerization. Insets show magnified images of corresponding capsules. (d) Reflectance spectra of photonic capsules shown in panels (a)−(c), where a single capsule is used for each reflectance measurement. Insets show optical microscope images of the corresponding capsules.

DOI: 10.1021/cm5043292
Chem. Mater. 2015, 27, 1014−1020

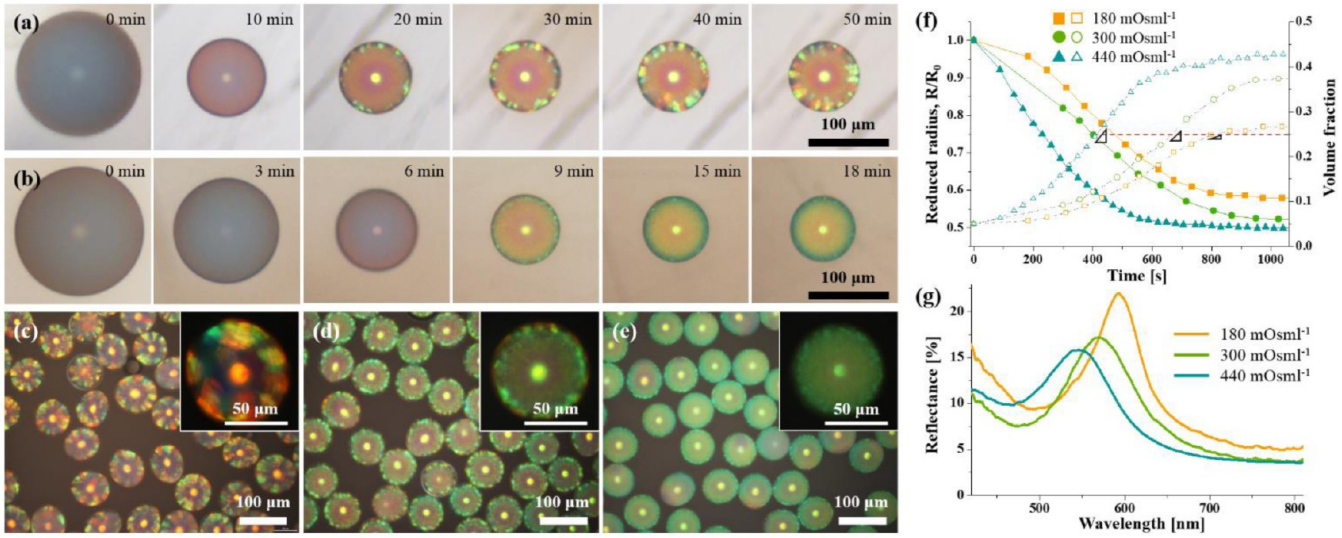

Figure 3. (a, b) Time series of optical microscope images showing the shrinkage of double-emulsion droplets containing PS particles with diameter of 191 nm incubated in aqueous solutions with osmolarities of (a) 180 mOsm L^{-1} and (b) 440 mOsm L^{-1}. The incubation time is denoted in each image. (c–e) Optical microscope images of photonic capsules prepared by incubation in aqueous solutions with osmolarities of (c) 180 mOsm L^{-1}, (d) 300 mOsm L^{-1}, and (e) 440 mOsm L^{-1}. Insets show magnified images of the corresponding capsules. (f) Time dependence of the reduced radius of double-emulsion droplets (filled symbols) and the concentration (empty symbols) of PS particles in the innermost droplets under the three different osmotic pressure conditions. Red dashed line indicates the volume fraction at the onset of crystallization and triangles indicate the concentration rates. (g) Reflectance spectra of corresponding photonic capsules.

$$\phi(t) = \phi_0\left(\frac{R_0 - l_0}{R(t) - l(t)}\right)^3 \tag{2}$$

where

$$l(t) = R(t) - \{R(t)^3 - {R_0}^3 + (R_0 - l_0)^3\}^{1/3} \tag{3}$$

To obtain the value of l_0, we intentionally rupture double-emulsion drops and calculate l_0 to be 0.20 μm from the volume of the resulting single oil drop.[12] The reduced radius of the drop (R/R_0) is plotted on the left y-axes of Figure 3f and the particle volume fraction on the right. At an osmolarity of 180 mOsm L^{-1}, the volume fraction of particles at the onset of crystallization is 0.248, as shown in Figure 3f. At the same volume fraction, the concentration rates, which are represented as slopes of curves, at 300 mOsm L^{-1} and 440 mOsm L^{-1}, are 2–3 times higher than that at 180 mOsm L^{-1}, suppress crystallization, and create different internal structures and optical properties. The final volume fractions vary from 0.296 at 180 mOsm L^{-1} to 0.428 at 440 mOsm L^{-1}. Such differences in the particle density result in variation of the structural resonance, as shown in Figure 3g. The sample prepared at 180 mOsm L^{-1} shows a sharp peak at a wavelength of 593 nm with a reflectivity of 22.0% and normalized full width at half-maximum (fwhm, $\Delta\lambda/\lambda$) of 0.102. From eq 1, we find a volume fraction of 0.295 for this sample, in good agreement with the value 0.296 obtained from eq 2. The sample prepared at 300 mOsm L^{-1} has a peak that is blue-shifted to 565 nm and a lower reflectivity of 17.7% and $\Delta\lambda/\lambda$ = 0.145. The reflectance spectrum of the sample prepared under 440 mOsm L^{-1} shows reflectivity of 15.8% at a resonance wavelength of 546 nm and $\Delta\lambda/\lambda$ = 0.144. We attribute the reduction of reflectivity and the broadening of the reflection peak to the formation of glassy internal structures.[10a] The resonance wavelength of the disordered structure deviates from eq 1; the equation predicts wavelengths of 554 nm for ϕ = 0.375 and 535 nm for ϕ = 0.428, which are slightly smaller than the observed peak positions of 565 and 546 nm. This indicates that the interparticle distance in the disordered structure is slightly larger than the spacing of (111) planes of an fcc lattice with the same volume fraction of particles.

Control of Internal Structures at Constant Volume Fraction. As our experiments show, the osmotic pressure gradient is the critical parameter that controls both the crystallinity and the wavelength of the structural resonance. This suggests that independent control of iridescence and color wavelength is difficult to achieve at a constant osmotic pressure. One way to control the internal structure at constant volume fraction of particles is to adjust the external osmotic pressure while the drop shrinks. Therefore, we investigate increasing the osmolarity of the incubation solution stepwise to slowly but steadily concentrate the sample to a high volume fraction. We use two different protocols to increase the external osmotic pressure on droplets containing a 5% v/v aqueous suspension of PS nanoparticles with D = 191 nm. In one protocol, we increase the osmolarity to 300 mOsm L^{-1} in one step. In the other protocol, we increase the osmolarity in three steps: to 100 mOsm L^{-1}, then to 180 mOsm L^{-1}, and then to 300 mOsm L^{-1}. We then monitor how the structural colors of the microcapsules develop under these two compression protocols; as shown in Figures 4a and 4b, the one-step compression leads to capsules with uniform color, while the stepwise compression leads to a sparkling color pattern (see Figures S1b and Figure S2 in the Supporting Information, and Movie S3 for full series of images). Although in each batch, the size and appearance of the microcapsules are consistent, the two batches differ qualitatively in appearance, as shown in the left panels of Figures 4c and 4d. Aqueous suspensions of these microcapsules reflect the same color of light but at different intensities, as shown in the right panels; in particular, the microcapsules prepared stepwise show brighter green reflection. We directly observe the internal structures of the two batches of microcapsules using scanning electron microscopy (SEM), as shown in Figures 4e and 4f; the microcapsules are cryogenically fractured prior to observation. In the microcapsules prepared in

DOI: 10.1021/cm5043292
Chem. Mater. 2015, 27, 1014–1020

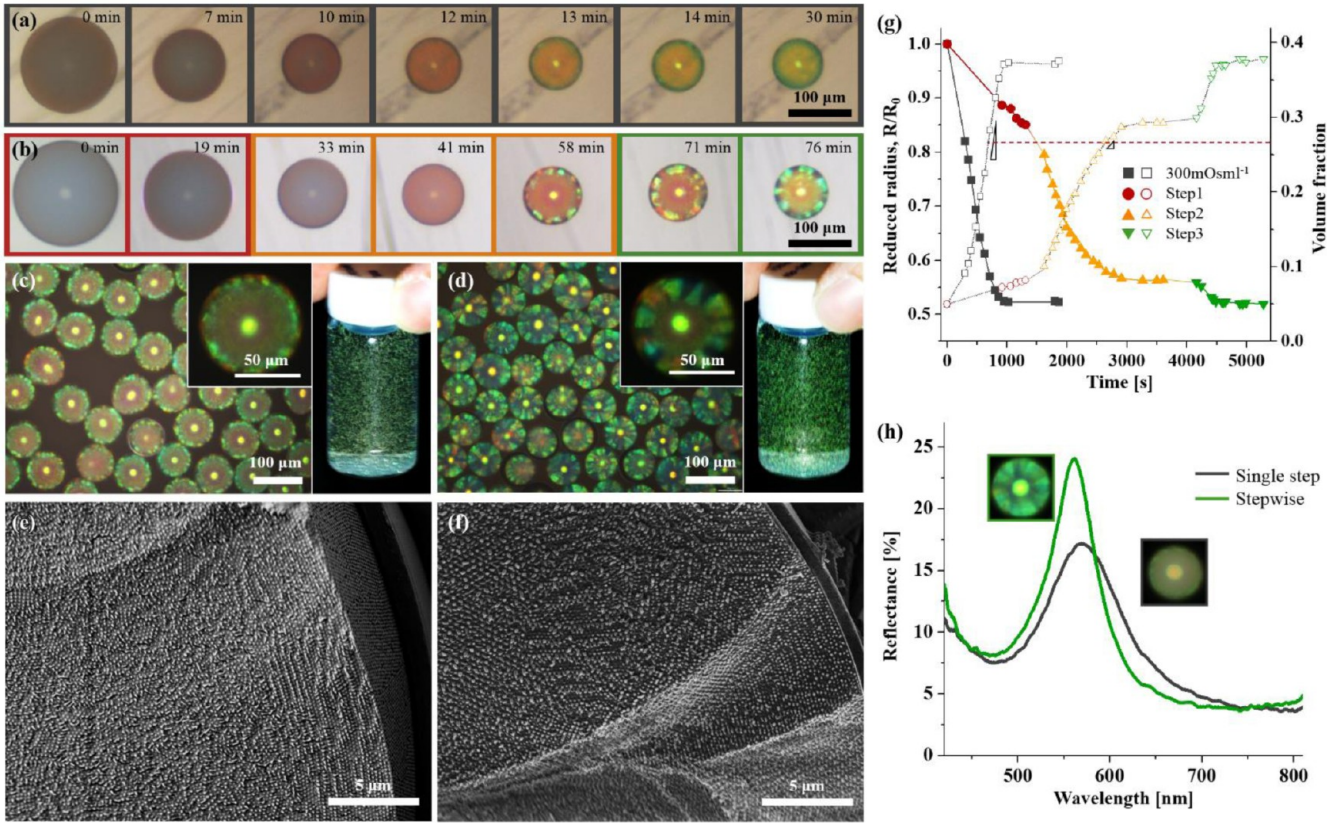

Figure 4. (a, b) Time series of optical microscope images showing the shrinkage of double-emulsion droplets with two different histories; the droplets in panel (a) are incubated in an aqueous solution with an osmolarity of 300 mOsm L^{-1}, whereas the droplets in panel (b) are incubated at 100 mOsm L^{-1} for 20 min (denoted by a red box), then at 180 mOsm L^{-1} for 40 min (denoted by an orange box), and finally at 300 mOsm L^{-1} for 30 min (denoted by a green box). The incubation time is denoted at each image. (c, d) Sets of optical microscope images and photographs of aqueous suspensions of the capsules prepared by single-step concentration (panel (c)) and stepwise concentration (panel (d)). (e, f) Cryo-scanning electron microscopy (Cryo-SEM) images showing the internal structures of photonic capsules prepared by single-step concentration (panel (e)) and stepwise concentration (panel (f)). (g) Time dependence of the reduced radius of double-emulsion droplets (filled symbols) and concentration (empty symbols) of PS particles in the innermost droplets at two different osmotic pressure conditions. Red dashed line indicates the volume fraction at the onset of crystallization and triangles indicate the concentration rates. (h) Reflectance spectra of corresponding photonic capsules. Insets are taken under the same exposure conditions.

one step, the particles form amorphous structures that extend from the center of the capsules to 5 μm from the inner wall, as shown in Figure 4e and Figure S3 in the Supporting Information; there is a layer of crystalline structure ~5 μm thick along the membrane. By contrast, microcapsules prepared stepwise have ordered structures throughout their entire volume, as shown in Figure 4f and Figure S4 in the Supporting Information. The (111) fcc plane forms along the inner wall of the capsule membrane. Based on the SEM and optical microscopy observations, we conclude that the structural colors of the photonic microcapsules can be controlled kinetically by altering the rate of compression under a constant osmotic pressure.

The kinetic control of the nanostructure can be understood by comparing the measured size of the droplets and the corresponding volume fraction as a function of compression time, as summarized in Figure 4g. In a step-by-step increase, the onset of crystallization is observed in the second step, at $t \approx 2650$ s (see Figure S2 in the Supporting Information), where the volume fraction of particles is 0.269, as shown in Figure 4g. At the same volume fraction, the concentration rate for a one-step increase is 6.26-fold higher and results in the formation of a glasslike structure. Because the final osmotic pressure in the surrounding fluid is identical for both paths, the reduced radius and volume fraction at equilibrium are also the same. This results in almost the same resonance wavelength for both microcapsules, as shown in Figure 4h. The distinctive optical properties of the two microcapsules are also shown in the reflectance spectra: the crystal has higher reflectivity at the resonance wavelength and a smaller fwhm value. This step-by-step increase of osmolarity can be applied to PS particles with D = 222 and 156 nm, which results in red and blue microcapsules containing crystalline phases, as shown in Figure S5 in the Supporting Information; a single-step increase yields comparable color but lower reflectivity.

To further study the differences in optical properties between microcapsules containing crystalline and glassy internal structures, we characterize the angle dependence of the resonance peak using a 100× objective lens in a microscope equipped with a fiber-coupled spectrometer.[10b] A single microcapsule, located in the center of the field of view, is displaced step-by-step from the center and its reflectance spectrum at each location is measured, as illustrated in Figure 5a. Because the reflectance spectrum of an off-center microcapsule has a contribution from off-normal incident and reflected light, the angle dependence of photonic microcapsules can be characterized by the shift in the reflectance peak during the displacement. For a microcapsule containing a glassy colloidal structure, the peak position blue shifts only ~10 nm along a displacement equal to the microcapsule radius, as shown in

DOI: 10.1021/cm5043292
Chem. Mater. 2015, 27, 1014−1020

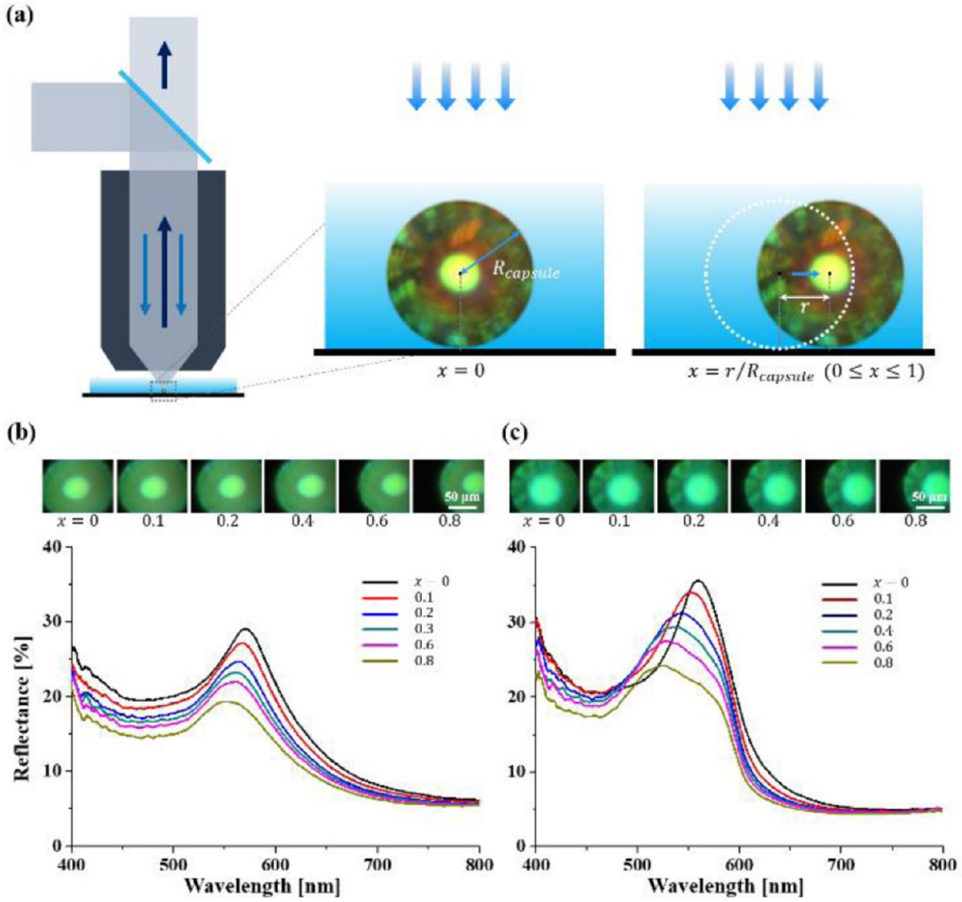

Figure 5. (a) Depiction of the setup used to measure reflection spectra from a single photonic capsule, where the capsule is displaced from the center to measure the angle dependence of the spectra; the displacement r is normalized to the capsule radius $R_{capsule}$ to yield the dimensionless displacement x. (b) Set of optical microscope images and reflectance spectra of a single photonic capsule containing a glassy packing of particles, where the value of x is adjusted from 0 to 0.8. (c) Same set of data obtained from a photonic capsule containing colloidal crystals.

Figure 5b. By contrast, a microcapsule containing a crystalline structure shows a blue shift as large as 40 nm for the same displacement, as shown in Figure 5c. Thus, our method also provides a means to control the iridescence, or angular dependence of the structural color, almost independently of the resonance wavelength.

CONCLUSION

We have shown that in microfluidically created double-emulsion drops, which serve as a spherical confining geometry for concentration of colloidal particles, the osmotic pressure of the surrounding fluid controls both the concentration rate of the particles inside the microcapsules and their equilibrium concentration. Therefore, the osmotic pressure influences both the internal arrangement of the particles and their interparticle distance at the same time. Independent control of the internal structure and interparticle distance can be achieved by precise control of the external osmotic pressure. Increasing the osmotic pressure step-by-step enables slow but steady concentration, allowing us to create crystalline structures at a high volume fraction of particles. These structures show a sparkling color pattern with strong iridescence. By comparison, a single-step increase of the osmotic pressure to the same final value used in the stepwise compression leads to a fast concentration that suppresses crystallization, thereby creating a glassy colloidal structure at the same volume fraction as the crystal. This amorphous structure exhibits homogeneous color across the microcapsule and no iridescence. Therefore, the resonance wavelength and degree of iridescence of the photonic microcapsules can be independently controlled. This precise control over optical properties provides new opportunities for making structurally colored paint pigments or photonic devices that use such microcapsules as building blocks. Furthermore, the internal photonic structure of the microcapsules can be designed to be stimulus-responsive, which may allow for the design of biosensors for subcutaneous injection.

EXPERIMENTAL SECTION

Materials. The polystyrene particles are synthesized by emulsion polymerization to have three different diameters: 156, 191, and 222 nm. Suspensions of such particles containing 2% w/w poly(vinyl alcohol) (PVA, Mw = 13 000−23 000) are used as the innermost phase in the microfluidic device. The middle oil phase is a photocurable resin of ethoxylated trimethylolpropane triacrylate (ETPTA, M_n ~428) containing 1% w/w photoinitiator, 2-hydroxy-2-methylpropiophenone. The continuous phase for drop generation is 10% w/w PVA, and the incubation solution for drop shrinkage is an aqueous solution of sodium chloride and 2% w/w PVA; the concentration of sodium chloride is adjusted to control the osmotic pressure. 2-[Methoxy(polyethyleneoxy)propyl]trimethoxyl silane is used to render glass capillaries hydrophilic and *n*-octadecyltrimethoxyl silane to render them hydrophobic prior to their assembly. All chemicals are purchased from Sigma−Aldrich except the hydrophilic silane

DOI: 10.1021/cm5043292
Chem. Mater. 2015, 27, 1014−1020

coupling agent, 2-[methoxy(polyethyleneoxy)propyl]-trimethoxyl silane, which is purchased from Gelest, Inc.

Fabrication and Operation of Microfluidic Device. Two cylindrical glass capillaries 1.00 mm in outer diameter are tapered with a capillary puller (Model P-97, Sutter Instruments), and their tips are carefully sanded off to have diameters of 100 and 200 μm. The capillary with a tip diameter of 100 μm is treated with *n*-octadecyltrimethoxyl silane to render the surface hydrophobic, and the capillary with a tip diameter of 200 μm is treated with 2-[methoxy(polyethyleneoxy)propyl]trimethoxyl silane to render the surface hydrophilic. The surface-modified capillaries are inserted through two opposite entrances of a square glass capillary 1.05 mm in inner dimension and are then coaxially aligned. Another small tapered cylindrical capillary is inserted into the wide opening of the hydrophobic capillary. The innermost phase is injected through the small tapered capillary, and the middle phase is injected through the hydrophobic capillary. The continuous phase is injected through the interstices between the hydrophobic and the square capillaries.

Drop Incubation. The double-emulsion drops are incubated in aqueous solutions of sodium chloride and PVA at room temperature, where the concentration of sodium chloride is controlled to achieve osmolarities of 100, 180, 300, and 440 mOsm L^{-1}; the osmolarities are confirmed by osmometer (Osmomat 030-d, Gonotec) measurements before use. After the drops are incubated for 2 h, a UV light (spot UV, INNO−CURE 100N) irradiates them for 2 min to photopolymerize ETPTA in the middle phase.

Characterization. Generation of double emulsions in a microfluidic device is observed using an inverted optical microscope (Eclipse TS100, Nikon) equipped with a high-speed camera (MotionScope M3, IDT). The images and reflectance spectra of the photonic capsules are taken using an optical microscope (Eclipse L150, Nikon) equipped with a fiber-coupled spectrometer (USB4000, Ocean Optics). The internal structures of the photonic microcapsules are observed with SEM (NVision dual focused ion beam, Zeiss). Prior to SEM observation, the microcapsules are quickly frozen in liquid nitrogen and knife-fractured. The samples are sputter-coated with Pt/Pd and then transferred into the SEM, using the vacuum cryo-transfer system (Model EM VCT100, Leica).

■ ASSOCIATED CONTENT

Ⓢ Supporting Information

Series of optical microscope images showing drop shrinkage under various osmotic pressure conditions, optical microscope images and photographs of photonic capsules, and cryo-SEM images showing internal colloidal structures are included in the Supporting Information. This material is available free of charge via the Internet at http://pubs.acs.org.

Ⓦ Web-Enhanced Features

Movies S1−S3 are included to show the production of monodisperse double-emulsion drops and their evolution under hypertonic conditions.

■ AUTHOR INFORMATION

Corresponding Author

*E-mail: kim.sh@kaist.ac.kr.

Notes

The authors declare no competing financial interest.

■ ACKNOWLEDGMENTS

This work was supported by the International Collaboration (Grant No. Sunjin-2010-002 from the MOTIE) and the Midcareer Researcher Program (No. 2014R1A2A2A01005813), through an NRF grant funded by the MSIP. This work was performed in part at the Center for Nanoscale Systems (CNS) in Harvard University, a member of the National Nanotechnology Infrastructure Network (NNIN), which is supported by the National Science Foundation (under NSF Award No. ECS-0335765). We thank Sofia Magkiriadou (Harvard University) for useful discussions.

■ REFERENCES

(1) (a) Marlow, F.; Muldarisnur; Sharifi, P.; Brinkmann, R.; Mendive, C. *Angew. Chem., Int. Ed.* **2009**, *48*, 6212. (b) Kim, S.-H.; Lee, S. Y.; Yang, S.-M.; Yi, G.-R. *NPG Asia Mater.* **2011**, *3*, 25. (c) Kinoshita, S.; Yoshioka, S. *ChemPhysChem* **2005**, *6*, 1442.

(2) Jiang, P.; Bertone, J. F.; Hwang, K. S.; Colvin, V. L. *Chem. Mater.* **1999**, *11*, 2132.

(3) (a) Ueno, K.; Inaba, A.; Sano, Y.; Kondoh, M.; Watanabe, M. *Chem. Commun.* **2009**, 3603. (b) Harun-Ur-Rashid, M.; Imran, A. B.; Seki, T.; Ishii, M.; Nakamura, H.; Takeoka, Y. *ChemPhysChem* **2010**, *11*, 579.

(4) (a) Holtz, J. H.; Asher, S. A. *Nature* **1997**, *389*, 829. (b) Weissman, J. M.; Sunkara, H. B.; Tse, A. S.; Asher, S. A. *Science* **1996**, *274*, 959. (c) Puzzo, D. P.; Arsenault, A. C.; Manners, I.; Ozin, G. A. *Angew. Chem., Int. Ed.* **2009**, *48*, 943. (d) Shim, T. S.; Kim, S.-H.; Sim, J. Y.; Lim, J.-M.; Yang, S.-M. *Adv. Mater.* **2010**, *22*, 4494.

(5) (a) Josephson, D. P.; Miller, M.; Stein, A. *Z. Anorg. Allg. Chem.* **2014**, *640*, 655. (b) Kim, S.-H.; Jeon, S.-J.; Jeong, W. C.; Park, H. S.; Yang, S.-M. *Adv. Mater.* **2008**, *20*, 4129.

(6) (a) Brugarolas, T.; Tu, F.; Lee, D. *Soft Matter* **2013**, *9*, 9046. (b) Moon, J. H.; Yi, G.-R.; Yang, S.-M.; Pine, D. J.; Park, S. B. *Adv. Mater.* **2004**, *16*, 605. (c) Kim, J.; Song, Y.; He, L.; Kim, H.; Lee, H.; Park, W.; Yin, Y.; Kwon, S. *Small* **2011**, *7*, 1163.

(7) (a) Zhao, X.; Cao, Y.; Ito, F.; Chen, H.-H.; Nagai, K.; Zhao, Y.-H.; Gu, Z.-Z. *Angew. Chem., Int. Ed.* **2006**, *45*, 6835. (b) Kim, S.-H.; Lee, S. Y.; Yi, G.-R.; Pine, D. J.; Yang, S.-M. *J. Am. Chem. Soc.* **2006**, *128*, 10897. (c) Velev, O. D.; Lenhoff, A. M.; Kaler, E. W. *Science* **2000**, *287*, 2240.

(8) (a) Kim, S.-H.; Jeon, S.-J.; Yang, S.-M. *J. Am. Chem. Soc.* **2008**, *130*, 6040. (b) Hu, Y.; Wang, J.; Li, C.; Wang, Q.; Wang, H.; Zhu, J.; Yang, Y. *Langmuir* **2013**, *29*, 15529.

(9) (a) Wang, J.; Hu, Y.; Deng, R.; Xu, W.; Liu, S.; Liang, R.; Nie, Z.; Zhu, J. *Lab Chip* **2012**, *12*, 2795. (b) Kanai, T.; Lee, D.; Shum, H. C.; Shah, R. K.; Weitz, D. A. *Adv. Mater.* **2010**, *22*, 4998.

(10) (a) Kim, S.-H.; Park, J.-G.; Choi, T. M.; Manoharan, V. N.; Weitz, D. A. *Nat. Commun.* **2014**, *5*, 3068. (b) Shirk, K.; Steiner, C.; Kim, J. W.; Marquez, M.; Martinez, C. J. *Langmuir* **2013**, *29*, 11849.

(11) Park, J.-G.; Kim, S.-H.; Magkiriadou, S.; Choi, T. M.; Kim, Y.-S.; Manoharan, V. N. *Angew. Chem., Int. Ed.* **2014**, *53*, 2899.

(12) Kim, S.-H.; Kim, J. W.; Cho, J.-C.; Weitz, D. A. *Lab Chip* **2011**, *11*, 3162.

(13) Kim, P. G.; Stone, H. A. *EPL* **2008**, *83*, 54001.

(14) Kim, S.-H.; Lim, J.-M.; Jeong, W. C.; Choi, D.-G.; Yang, S.-M. *Adv. Mater.* **2008**, *20*, 3211.

(15) (a) Ballato, J.; Dimaio, J.; James, A.; Gulliver, E. *Appl. Phys. Lett.* **1999**, *75*, 1497. (b) Emoto, A.; Fukuda, T. *Appl. Phys. Lett.* **2012**, *100*, 131901.

DOI: 10.1021/cm5043292
Chem. Mater. 2015, 27, 1014−1020